



# Experimental measurement of wind turbine performance through Blade Element Theory

David Johnson, Ahmed Abdelrahman

Wind Energy Group

Department of Mechanical and Mechatronics Engineering



## Introduction

Experimental studies of turbine performance over realistic controlled conditions and at a scale that may be useful for modeling, validation and design are not common due to the required scale of both the turbine and the test facility. Testing wind turbines under controlled conditions allows advancement of understanding of rotor aerodynamics through the development of a documented experimental database, evaluation of existing standard predictive models and development of improved models. Wind turbine performance may be predicted analytically by the use of a simplified model outlined in well-developed rotor disc theory [1]. This model requires operating conditions and rotor geometries to estimate how the flow field is affected by the presence of the rotor. If, during field operation, the required flow field information was determined then an estimate of turbine performance could be made using the same method as the analytical approach. Model development requires good experimental measurements with well documented, unobstructed conditions on a reasonable size turbine.

The blade element momentum (BEM) method can also be used to determine the thrust and power of a wind turbine for chosen operating conditions. A typical representation of the vectors and forces on an element are shown in Figure 1 where  $\Omega r(1+a')$  is the rotor angular velocity, and  $W$  is the resultant relative velocity. To calculate the coefficient of power, a key measure of performance, using the BEM approach requires the operational conditions, geometry of the rotor, and the induction factors. The induction factors are a measure of the degree to which the flow is altered due to the presence of the rotor. The axial and tangential induction factors are derived in terms of the axial and tangential velocities immediately behind the rotor. (See 'Equations').

## EXPERIMENTAL SETUP

The wind facility which was used in all experiments is an open circuit tunnel with six identical fans driving the flow in a 3x2 arrangement. Each fan generates air flow of 78.7 m<sup>3</sup>/s at 413.5 Pa. The fans discharge into a 8.23 m long by 8.54 m wide by 5.9 m high plenum. The fan exit plane is rectangular with an 8.0 m width and 5.9 m height as can be seen upstream of the turbine in Figure 2.

The turbine utilized in these studies was a purpose built 1.5kW nominal, 3 bladed 3.3 m diameter horizontal axis wind turbine. The wind turbine test apparatus is comprised of: the tower, nacelle, blades, generator and the drivetrain. The hub height is 3.1 m above the ground.

The sonic anemometer was mounted on a separate tower at hub height behind the rotor; approximately 8.1m downstream of the fan plenum exit and 3.1m above the floor plane. The measurements were obtained 10 to 12 cm behind the rotor plane due to physical constraints caused by the geometry of the sonic anemometer as shown in figure 3.

## IMAGES

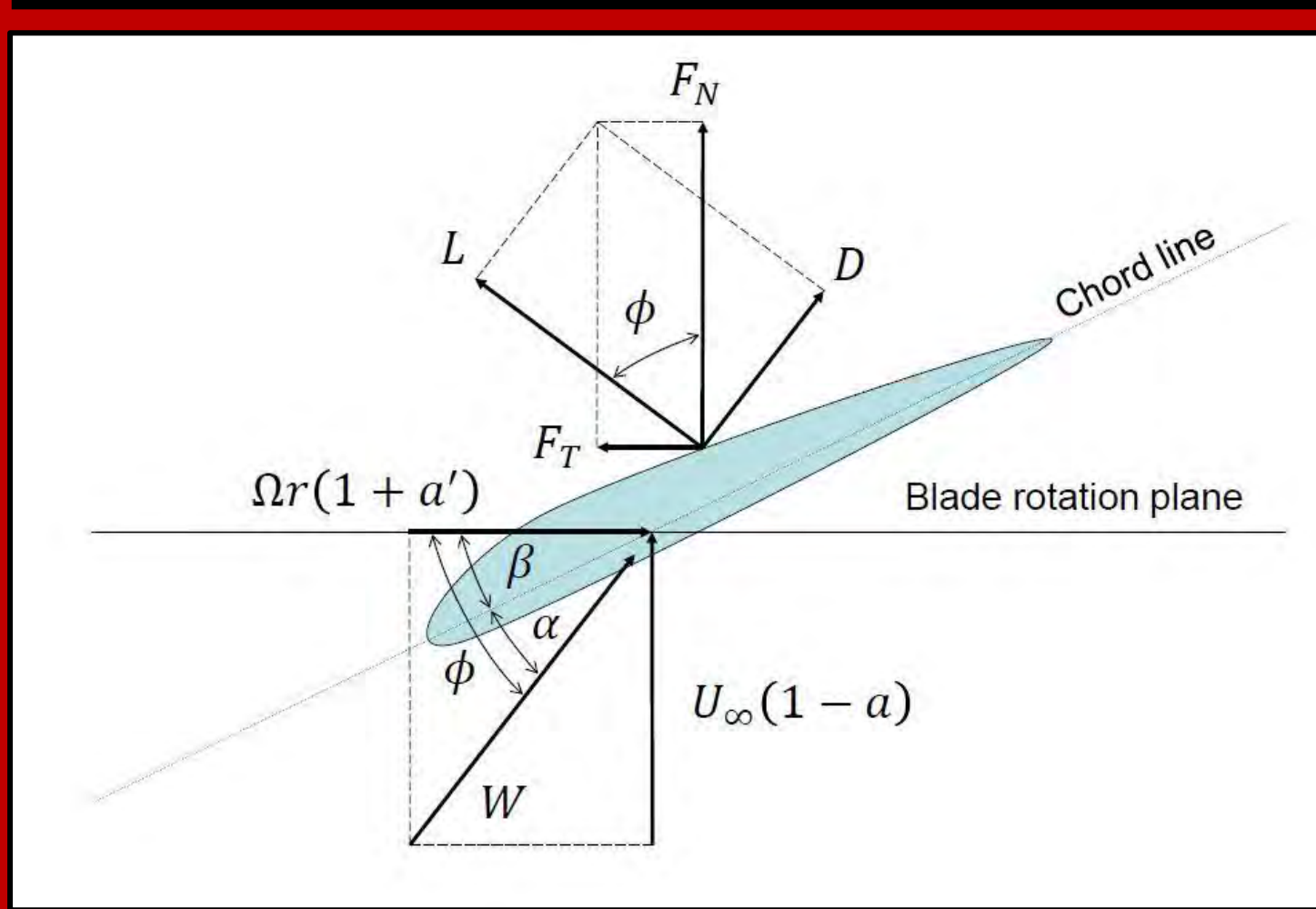


Figure 1: Velocity, force and geometric parameters for a blade element.



Figure 2: Anemometer traverse and wind turbine (looking upstream)



Figure 3: Three component sonic anemometer and blade orientation showing typical clearance.

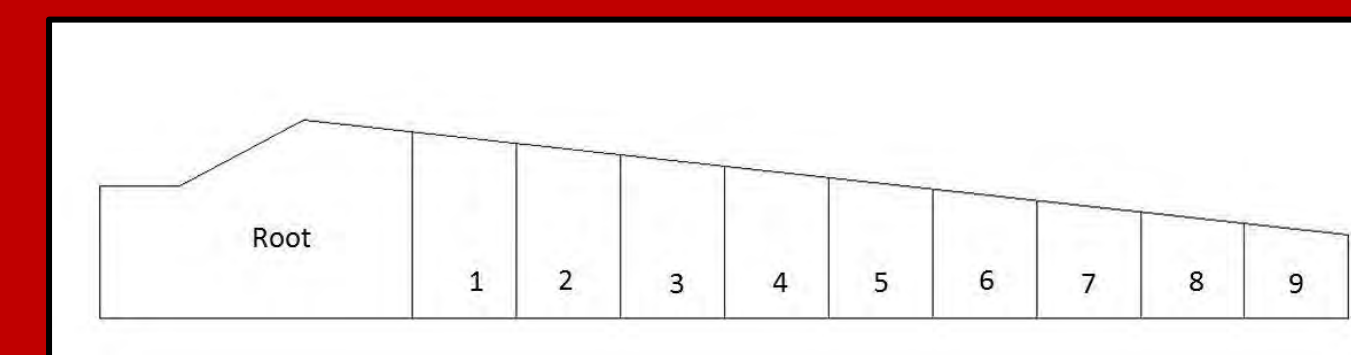


Figure 4: Plan view of turbine blade showing blade elements and measurement locations..

## Equations

$$C_{p_i} = \frac{8(1 - (a)_r) a'_r r^3 \Omega^2}{R^2 U_\infty^2} dr \quad \lambda = \frac{\Omega R}{U_\infty}$$

$$(a')_r = \frac{(U_\theta)_r}{2\Omega r} \quad (a)_r = 1 - \frac{(U_x)_r}{U_\infty}$$

$U_\theta$   $\equiv$  tangential velocity behind rotor  
 $U_x$   $\equiv$  axial velocity behind rotor  
 $U_\infty$   $\equiv$  free stream velocity  
 $a'$  and  $a$   $\equiv$  tangential and axial induction factors respectively

## PLOTS

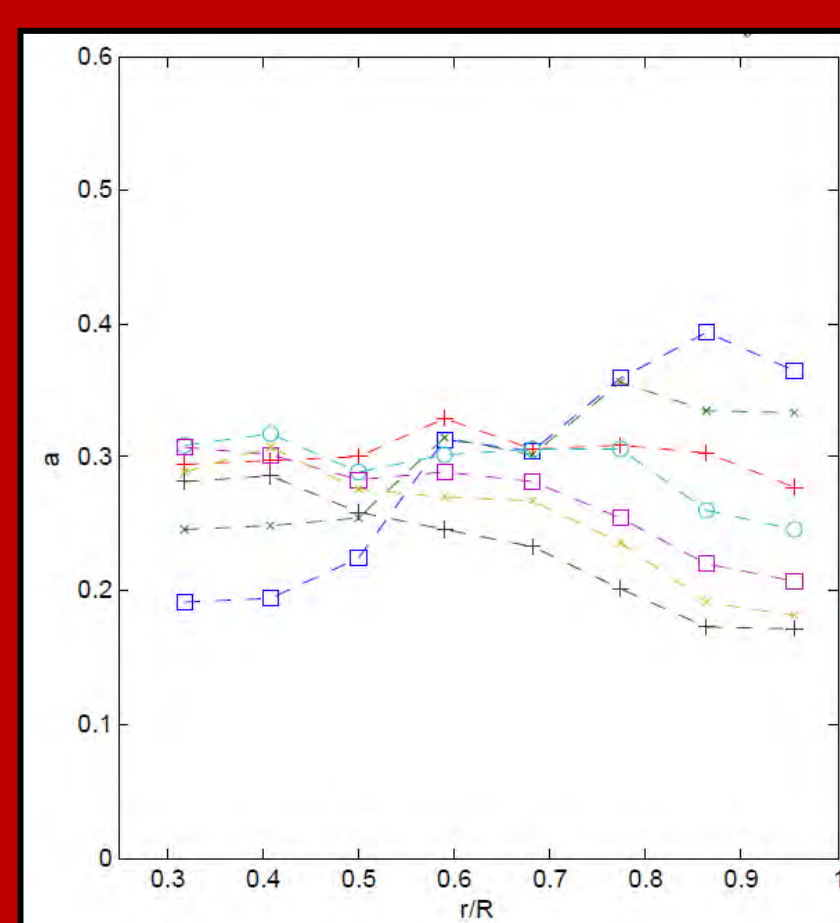


Figure 4 : Distribution for the axial inductions as a function of r/R for different tip speed ratios. \*\*design point. (see figure 5 for legend)

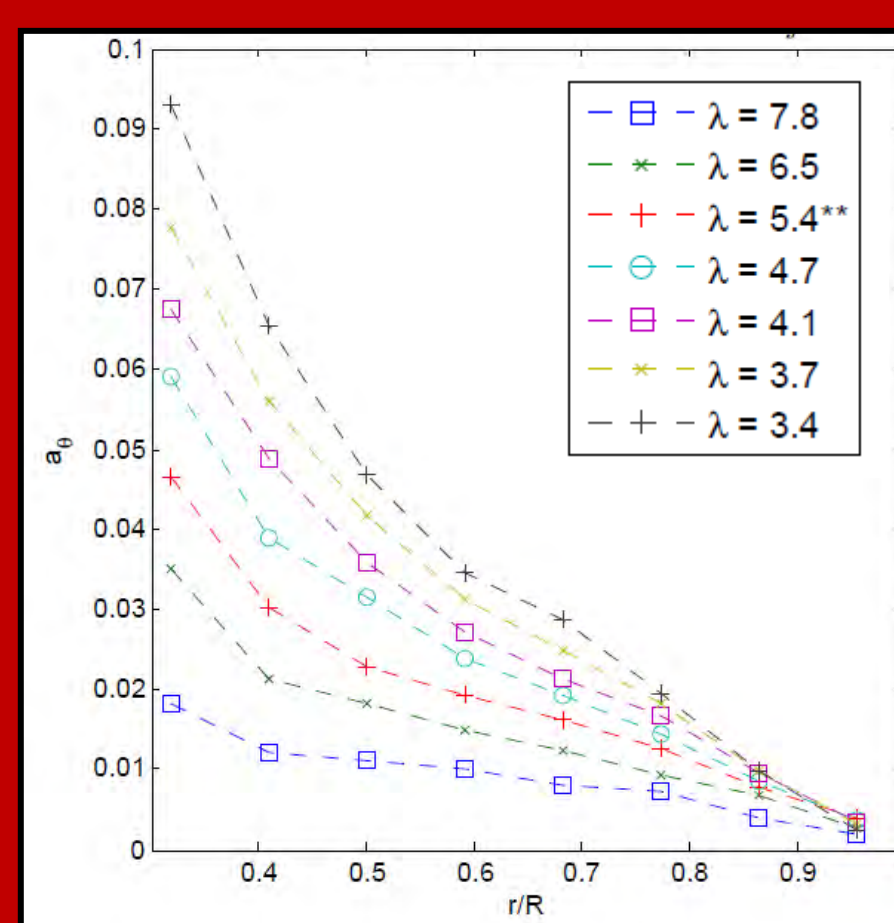


Figure 5 : Distribution for the tangential inductions as a function of r/R for different tip speed ratios. \*\*design point.

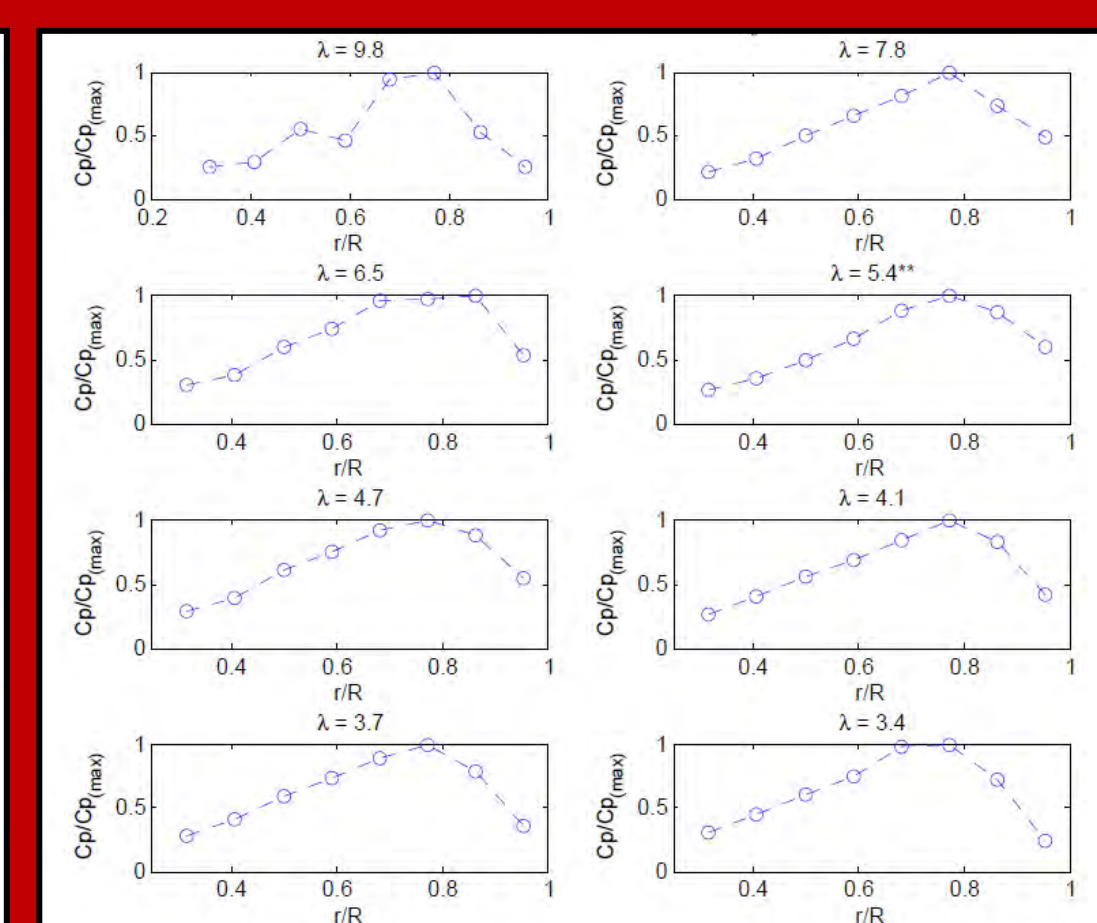


Figure 7: Distribution of  $C_p/C_{p(max)}$  versus r/R. \*\* design point.

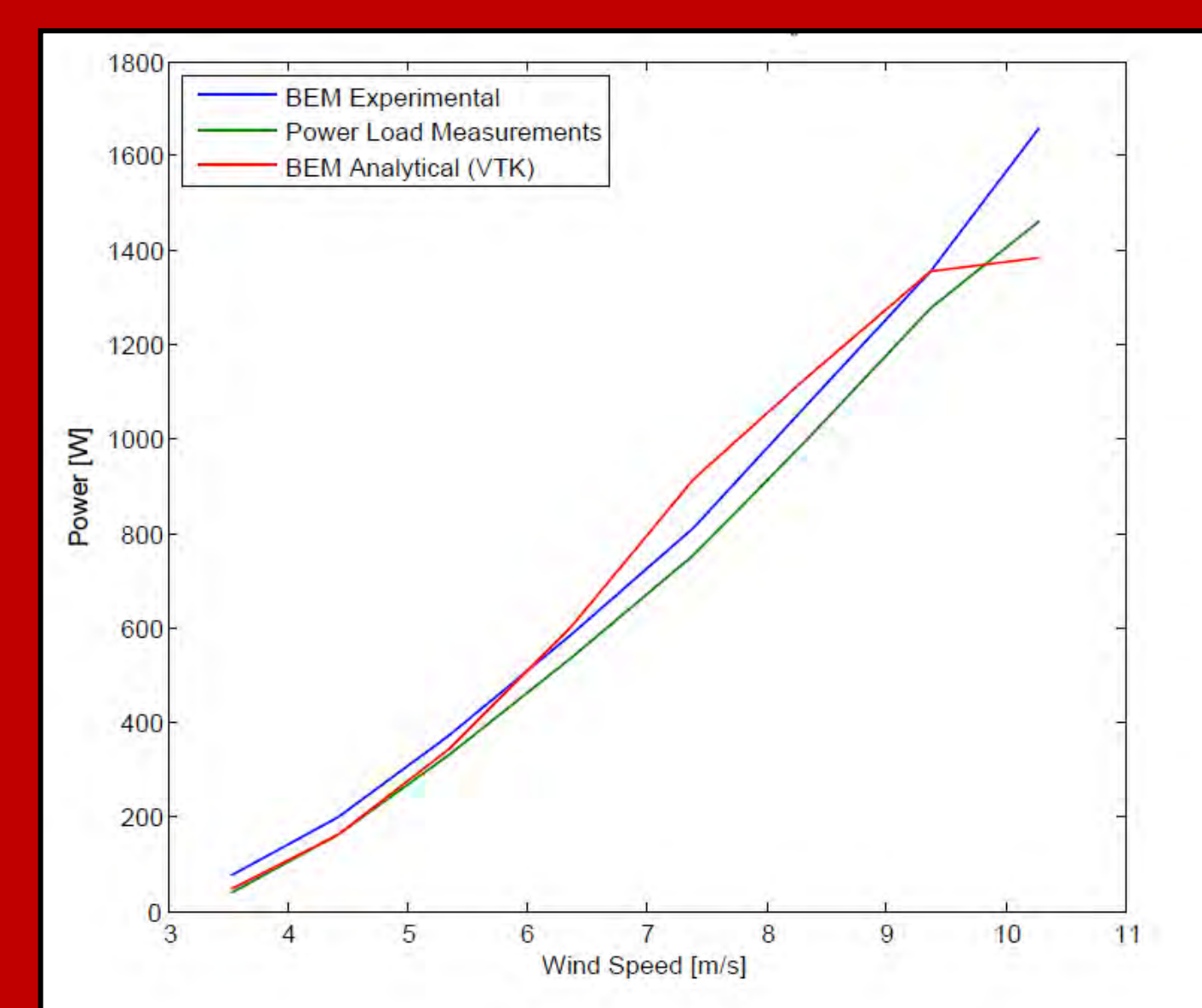


Figure 6: Turbine power output as a function of Wind Speed. Power load and analytical BEM data from [2].

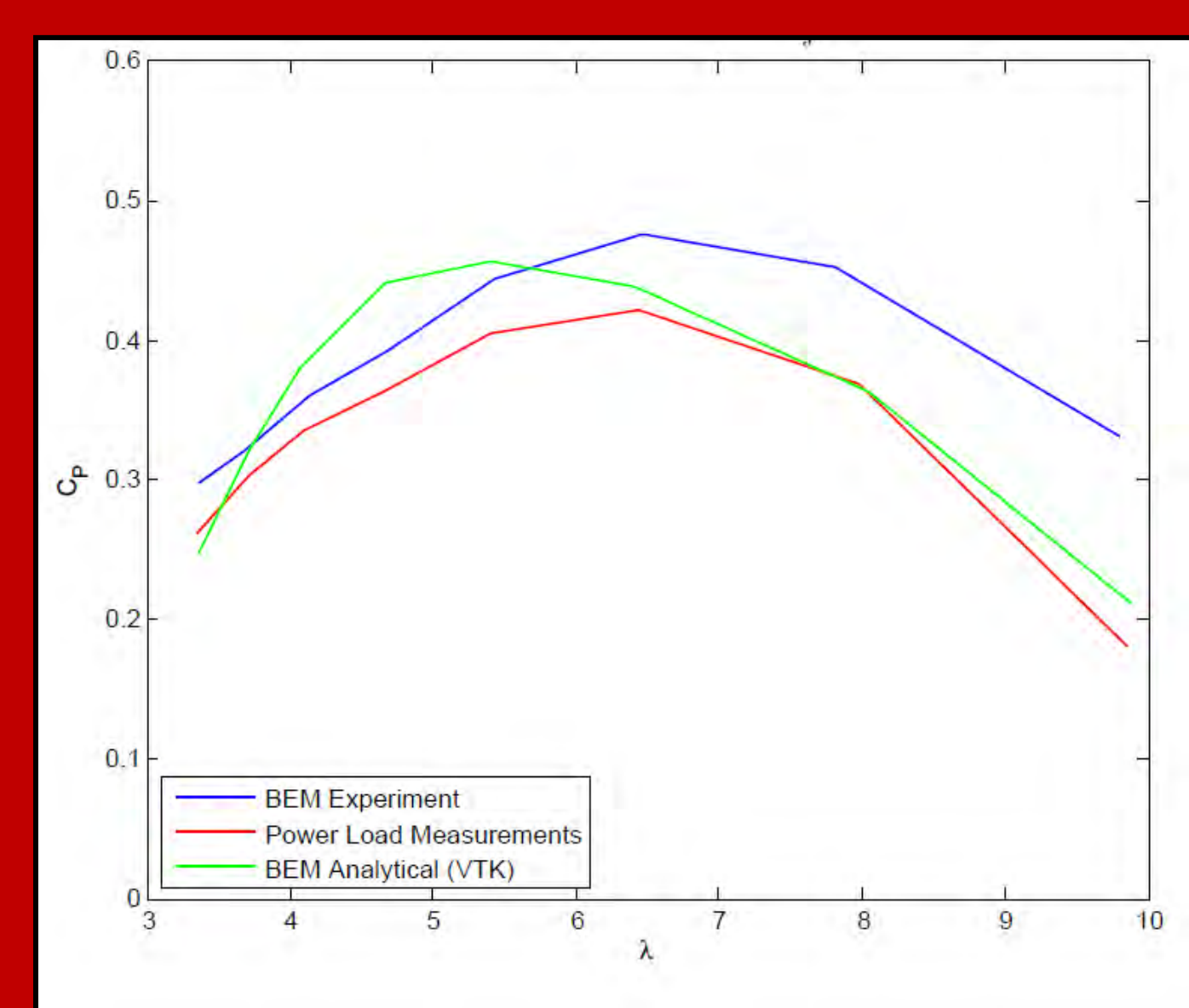


Figure 8: Distribution of  $C_p$  versus  $\lambda$ . Power load and analytical BEM data from [2].

## References

1. M. Hansen, Aerodynamics of Wind Turbines, Earthscan Sterling, VA, 2008. Gertz, Drew, "An Evaluation Testbed for Alternative Wind Turbine Blade Tip Designs" Master's thesis, University of Waterloo, 2011.
2. D. Gertz, D. Johnson, An evaluation testbed for wind turbine blade tip designs baseline case, International Journal of Energy Research 35 (2011) 1360-1370.

## TESTING

- Eight free stream wind velocities ( $U_\infty$ ) were chosen, between 3.5 and 10.3 m/s, while the rotor was fixed at 200 rpm.
- 3 component Velocity measurements were collected at 60Hz behind the rotor in the center of each of the 8 blade elements shown in figure 4 (elements 2 to 9).
- A 3.6 kW DC motor/generator was used as the basis for the electrical design and for the rotor speed control. The power produced/absorbed was determined through voltage and current measurements at the DC motor and a load bank.

## EXPERIMENTAL RESULTS

**Axial Induction Distributions ( $a_r$ ) (Figure 4):** Close to the design condition ( $\lambda = 5.4$ ) ( $a_r$ ) is fairly uniform in the region of 0.3 with a slight reduction as the tip is approached. No significant variation is observed in the values as  $r/R$  approaches 1. At low  $\lambda$  values (high  $U_\infty$ ) the region is characterized by low values of ( $a_r$ ) which indicate the overall flow is less impacted by the presence of the turbine.

**Tangential Induction Distributions ( $a'_\theta$ ) (figure 5):** The distribution shows increasing ( $a'_\theta$ ) with decreasing  $\lambda$  values and a decrease in ( $a'_\theta$ ) with increasing  $r/R$  values for all  $\lambda$  values. ( $a'_\theta$ ) becomes significant as  $\lambda$  decreases due to the vortex formed at the root.

**Power Production (figure 6):** The measured power for the turbine over the range of measured wind speeds is shown along with the predicted and independent power generation data from Gertz and Johnson[2] for the same blade and turbine. There is close agreement with the measured power data with this method indicating higher values over all wind speeds.

**$C_p$  Distribution (figure 7 and 8):** The radial  $C_p$  distribution displayed some of the expected characteristics including root and tip losses as can be seen in Figure 7. The highest performance is found at  $r/R = 0.77$  for the majority of the  $\lambda$  cases. Peak performance is found at  $\lambda = 6.5$ , the value with three radial values close to  $C_{p(max)}$ . The produced  $C_p$  vs.  $\lambda$  relation is shown in figure 8 and compared with modeling and independent power generation data from Gertz and Johnson[2]. The values determined using this approach parallel the measured power results with a clear over prediction over the entire range attributed to the discrete segment approach.

## CONCLUSIONS

The rotor performance determined with this method closely followed electrical turbine power measurements despite BEM assumptions. The details of these results should be useful to further understand the flow immediately downstream of a rotor in controlled conditions and provide detailed data for BEM model enhancement and future model development.